

Organic-Inorganic Hybrid Materials. 2. Compared Structure of Polydimethylsiloxane and Hydrogenated Polybutadiene Based Ceramers

Françoise Surivet

Centre de Recherches Corning Europe, 7 bis avenue de Valvins, 77 211 Avon Cedex, France

Thanh My Lam* and Jean-Pierre Pascault

Laboratoire des Matériaux Macromoléculaires—URA CNRS 507, Institut National des Sciences Appliquées de LYON, 20, avenue Albert Einstein, 69621 Villeurbanne Cedex, France

Christian Mai

GEMPPM—URA CNRS 341—Institut National des Sciences Appliquées de LYON, 20, avenue Albert Einstein, 69621 Villeurbanne Cedex, France

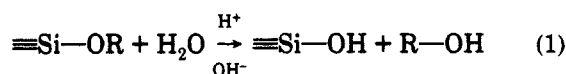
Received March 16, 1992

ABSTRACT: Different ceramer networks were successfully prepared in bulk or in solution. High transparency was observed for all the samples based on hydrogenated polybutadiene (H-PBD) and polydimethylsiloxane (PDMS) oligomers. These materials are microphase-separated materials due to the thermodynamic incompatibility between the different constitutive units. A similar microstructure exists in both types of samples: silicate clusters (or more precisely, polysiloxane clusters) including the cross-link points are dispersed in the oligomer-rich phase. In the case of PDMS ceramers, the three types of constitutive units are immiscible, so the morphology of such materials may be described by a three-phase system including the soft phase, practically pure in PDMS, the silicate clusters, and an interfacial region containing the urethane-urea units. The structure of the polymer obliged this mixed phase to be between the soft and the hard segments. For H-PBD ceramers, the soft segments and the urethane-urea units are miscible, and a two-phase model may schematize the H-PBD ceramer structure. In every case, good correlation was observed between the clusters separation distances and the end-to-end distance of the oligomers. These schematic models are consistent with our experimental results: they explain the existence of a periodicity in the networks and the fact that the correlation distance increases with increasing oligomer length.

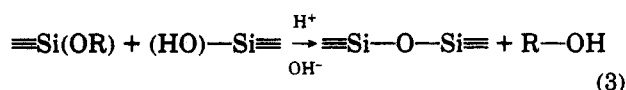
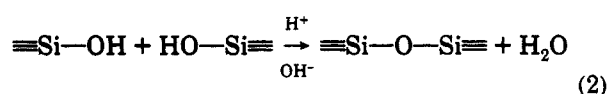
Introduction

The polymerization of metal alkoxides to produce glasses is commonly referred to as the sol-gel process. More recently, the sol-gel process has been used to create novel hybrid organic-inorganic networks, also called ceramers. Investigations on this kind of chemistry were focused on the use of silicon alkoxides $\text{Si}(\text{OR})_4$ and on the use of silane-terminated macromonomers $\text{MSi}(\text{OR})_3$.¹⁻³

Alkoxysilane groups react through a two-stage mechanism.⁴ (i) The first stage is hydrolysis which can be written as



(ii) The second stage is condensation, of which there are two kinds of reactions: water and alcohol-producing condensation



Reactions of tetraalkoxysilanes or trialkoxysilane-terminated macromonomers are similar and give siloxane $-\text{Si}-\text{O}-\text{Si}-$ bonds. The incorporation of organic compo-

nents (elastomers in particular) would hopefully impart flexibility to the inorganic glasses. They would make the manufacture of crack-free monolithic structures possible which could be, in principle, heat treated to obtain ceramics or used as modified materials in electrical, structural, or coating applications. Although these organic-modified networks will not be considered as conventional sol-gel glasses, they do represent a new group of hybrid materials. They should show some characteristics of the inorganic glassy network and also some properties of the organic species. Furthermore, it may also be possible that materials with special properties can be produced by choosing appropriate organic species.

Schmidt^{5,6} has reported several types of organic modifications to the sol-gel process. One example is the coupling of oligomeric species terminated with functional groups; one functional group reacts with the metal alkoxide, while the other containing an allyl or a vinyl group could later undergo a radical or an ionic reaction. Another application of this process is the synthesis of a solid polymer electrolyte (SPE).⁷⁻⁹ The sol-gel condensation of TEOS in the presence of poly(ethylene oxide) gives a polyether-silicate hybrid, which has been recognized as an excellent matrix of SPE. One important group of hybrid materials studied was based on TEOS and polydimethylsiloxane with silanol terminal groups.¹⁰⁻¹³ These materials showed some degree of phase separation of the PDMS component. However, the dispersion of the siloxane oligomer into the alkoxide-based material could be enhanced by higher levels of the acid catalyst or the use of a polymeric acid such as the catalyst.¹⁴ When PDMS oligomers were replaced by triethoxysilane-end-capped

* To whom all correspondence should be addressed.

poly(tetramethylene oxide) (PTMO) oligomers,^{15,16} the mechanical strength of these materials improved compared to the PDMS systems. No pure PTMO phase was observed, the dispersion of the oligomer was better in this case. The incorporation of oligomeric compounds can be enhanced by the presence of additional functional groups along their backbone: PTMO-based polyurethane oligomers with multiple triethoxysilane groups on their backbone¹⁷ were incorporated into a TEOS-based network. Due to the additional constraints caused by the triethoxysilane groups, the mobility of the oligomers decreased and the glass transition temperatures of the main phase increased. This results in a more glassy final material, and therefore these materials show significant improvement in both tensile modulus and strength. Oligomeric species that are glassy in pure form at ambient conditions can also be incorporated into hybrid networks, in addition to those possessing a more rubberlike backbone such as PDMS or PTMO. Indeed, materials incorporating triethoxysilane-functionalized poly(ether ether ketone)¹⁸ (PEEK) oligomers have been successfully made through a sol-gel reaction with TEOS.

The mechanical and physical properties of ceramers are a function of their thermal history, as reported by Huang et al.¹⁷ One explanation of the time-dependent behavior of the ceramer networks is based upon the time-temperature transformation (TTT) model proposed by Gillham et al.¹⁹ for thermosets. It is well-known that when a thermoset system cures, two principal structural transitions may occur: gelation and vitrification. Gelation marks the transition from a liquid to a rubbery state, since the cross-linked network has elastic properties not present in the low-molecular-weight, linear or branched prepolymers. Vitrification involves a transition from the liquid or rubbery state into the glassy state as a consequence of an increase in molecular weight before gelation or an increase in cross-link density after gelation. Chemical cross-linking does not necessarily stop after gelation; the chemical reaction may continue toward completion. Hence, given sufficient time, a network-forming system will continue to cross-link after gelation until all reactive sites are spent or vitrification occurs, quenching mobility. Though vitrification, like gelation, does not necessarily terminate the chemical cross-linking, the diffusion limitation is so great that additional reaction in a vitrified material can generally be ignored. Once vitrified, large scale molecular motions are not possible in this system; therefore, reactive sites can no longer come together and the chemical cross-linking reaction is effectively quenched. Time and thermal treatments at a temperature higher than the initial vitrification temperature will further the process. These changes with time in the ceramers are related to an increase in the connectivity of the network which would support higher stresses, as has been demonstrated for numerous ceramers.

As we have seen, the approach used extensively by many workers consists in copolymerization of tetraalkoxides with different oligomeric components. The goal of this work was to synthesize such hybrid materials without incorporating inorganic precursors. The ceramer networks will result in homopolymerization of alkoxy-silane-terminated macromonomers. These macromonomers are prepared by reacting two types of components: an organic-functionalized prepolymer and an organosilane $R_n\text{-Si-X}_{4-n}$, with two classes of functionalities. X is a hydrolyzable group able to be involved in inorganic reactions, and R is a nonhydrolyzable organic radical that possesses a functionality which enables the organosilane to react with the organic prepolymer. Our products were obtained through the reaction of (γ -aminopropyl)triethoxysilane with iso-

cyanate-terminated prepolymers. These isocyanate-functionalized prepolymers were prepared, in turn, from classical α,ω -hydroxy-terminated prepolymers and isophorane diisocyanate using the stoichiometry ratio calculated to give a level of excess isocyanate functionality such that all prepolymer molecules are isocyanate end-capped. The chemistry and composition of the final macromonomers were described in a previous publication.²⁰ Macrodiols chosen in this work were polydimethylsiloxane and hydrogenated polybutadiene oligomers.

The unique properties of siloxane polymers have led to their widespread application in many diversified fields. The outstanding properties of PDMS include their extremely low glass transition temperature (-123°C), high thermal oxidative stability, UV resistance, low surface energy and hydrophobicity, good electrical properties, and high permeability to many gases. Because of their biocompatibility and low toxicity, PDMS are also used in many biomedical applications.²¹ However, because of its poor mechanical properties, many of its initial potential applications have suffered in terms of performance. On the other hand, hydrogenated 1,2-polybutadiene-based polyurethanes offer the advantage of low moisture permeability, especially for adhesives and electrical coating applications, and they also offer a better resistance to oxidation.²²

The aim of this work is to investigate the thermal, mechanical, and structural properties of different ceramers. For that, we use alkoxy-silane-terminated macromonomers. The hydrolysis and condensation mechanisms involved in these systems were investigated in a previous paper.²³ In this study, the effects of the nature and the molecular weight of the macrodiol and of the curing process will be discussed. The dynamic mechanical properties of these hybrid materials will be reported, and the structural information obtained from small-angle X-ray scattering (SAXS) analysis will be provided.

Experimental Section

Starting Reagents. The formulas, molecular weights, and suppliers of the different materials are listed in Table I. The various products were used as received. α,ω -Hydroxyl-terminated oligomers were degassed at 60°C for 48 h before use. The catalysts used for alkoxy-silane reactions are trifluoromethanesulfonic acid (triflic acid), $\text{CF}_3\text{SO}_3\text{H}$, and hydrochloric acid, HCl.

Synthesis of α,ω -Silane-Terminated Macromonomers Based on Oligomers. Different types of macromonomers were prepared for testing. These silane-functionalized prepolymers were prepared via a two-step reaction.²⁰ In the first step, one mole of macrodiol reacted with two moles of diisocyanate in order to have a stoichiometric ratio $\text{NCO}/\text{OH} = 2$, in bulk at 80°C for 4 h under vacuum. At this time, size exclusion chromatography (SEC) of the materials showed no further change in the diisocyanate peak. In the second step, the product prepared above was dissolved in tetrahydrofuran (10^{-2} mol for 100 mL), the solution was immediately combined with the aminosilane with a stoichiometric ratio $\text{NCO}/\text{NH}_2 = 1$, and the mixture was stirred at room temperature for 1 h. An IR spectrum of the products showed no unreacted isocyanate and a complete reaction. The solvent was removed under a rotating evaporator at 40°C for 15 h. The characteristics of these α,ω -alkoxy-silane-terminated macromonomers are reported in Table II.

Synthesis of α,ω -Alkoxy-silane-Terminated Macromonomers Based on the Polyurethane Prepolymer. To increase the molecular weight of macromonomers, a reaction is carried out between diisocyanate and an excess of macrodiol in bulk for 4 h at 80°C under vacuum, in order to obtain a polyurethane prepolymer with an excess of hydroxyl groups. Two different stoichiometric ratios have been studied: $\text{NCO}/\text{OH} = 0.5$ and $\text{NCO}/\text{OH} = 0.66$.

Then, new diisocyanate was added with a stoichiometric ratio $\text{NCO}/\text{OH}_{\text{residual}} = 2$ (the percentage of residual hydroxyl groups

Table I
Characteristics of the Different Monomers Used

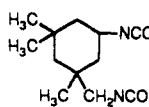
monomer	formula	mol wt	glass transition temp (°C)	supplier
α,ω -hydroxy-terminated polydimethylsiloxane (PDMS)	$\text{HO}-(\text{CH}_2)_3-\text{Si}(\text{CH}_3)_2-\text{O}-\text{Si}(\text{CH}_3)_2-(\text{CH}_2)_3-\text{OH}$	850 1950	-118 -125	Goldschmidt Goldschmidt
α,ω -hydroxy-terminated hydrogenated polybutadiene (H-PBD)	$\text{HO}-(\text{CH}_2-\text{CH}(\text{C}_2\text{H}_5)-\text{CH}_2-\text{CH}_2-\text{CH}_2-\text{CH}_2)_y-\text{OH}$	1550 2100 3100	-46 -45 -43	Nippon Soda Nippon Soda Nippon Soda
isophorone diisocyanate (IPDI)		222	-99	Aldrich
(γ -aminopropyl)triethoxysilane (γ -APS)	$\text{NH}_2-(\text{CH}_2)_3-\text{Si}(\text{OC}_2\text{H}_5)_3$	221	-130	Aldrich

Table II
SEC Characteristics of α,ω -Alkoxy-silane-Terminated Macromonomers

reference	PDMS or H-PBD	NCO/OH ^a	\bar{M}_n	I_p	\bar{M}_{th}
PU PDMS (4100)	1950	0.5	4100	2.1	5260
PU PDMS (6100)	850	0.67	6100	2.1	7700
PU PDMS (12 500)	1950	0.67	12500	2.1	14600
PU H-PBD (8200)	1000	0.67	8200	2.2	8350
PU H-PBD (14 000)	2000	0.67	14000	2.7	15800

^a Stoichiometric ratio used at the beginning of the first step.

was determined by chemical titration). The reaction continued for 4 h at 80 °C under vacuum.

These isocyanate-functionalized prepolymers prepared above were dissolved in tetrahydrofuran (10^{-2} mol for 100 mL) and the solution was immediately combined with the aminosilane with a stoichiometric ratio $\text{NCO}/\text{NH}_2 = 1$. The different mixtures were stirred at room temperature for 1 h. The solvent was removed under a rotating evaporator at 40 °C for 15 h. The characteristics of these α,ω -alkoxy-silane-terminated macromonomers are reported in Table II.

Synthesis of Ceramer Networks. Two types of synthesis were investigated: in bulk or in solution. In bulk, α,ω -alkoxy-silane-terminated macromonomers were rapidly mixed with amounts of deionized water and triflic acid at room temperature. Hydrolysis and condensation reactions were performed with 3 mol of H_2O to 1 mol of silane $3\text{H}_2\text{O}/\text{Si}$ and a ratio $\text{H}^+/\text{Si} = 0.05$. The blend was cast into a mould at 80 °C and cured for 12 h at this temperature under a pressure of 100 bars. The film thickness was about 1 mm.

For solution polymerization, α,ω -alkoxy-silane-terminated macromonomers were first dissolved in THF. The total concentration of polymer in THF was about 10% by weight. Then, a mixture of water and acid (in the same proportions as previously) was added under mixing. The solution was cast on glass dishes at room temperature and the gel was dried under ambient conditions for at least 2 weeks prior to testing.

Nomenclature. The nomenclature that was developed in this work can be illustrated by these two examples: PU PDMS (6100), PDMS (850). First, we indicate the type of oligomer or the prepolymer used as the soft sequence, followed by approximate molecular weight of the oligomer or the prepolymer.

The soft segment content was defined by using the common definition used for polyurethanes. It was taken equal to the mass of macrodiol divided by the total mass (macrodiol + organosilane + diisocyanate).

Characterization. The analyses of the soluble products were made on a Waters chromatograph equipped with a 6000A pump, U6K injector, double detection (UV at $\lambda = 254$ nm and differential refractometer (R401)). The eluants used were tetrahydrofuran (THF) and chloroform (CHCl_3), and the separation was carried out on four μ Styragel columns ($10^5 \text{ \AA} + 10^4 \text{ \AA} + 10^3 \text{ \AA} + 5 \times 10^2 \text{ \AA}$) with an elution rate of 1.5 mL/min. The approximate average molecular weights (\bar{M}_n , \bar{M}_w) were calculated using a polystyrene calibration.

A Mettler INC (TA 3000) microcalorimeter was used for the differential scanning calorimetry (DSC). Temperature and

enthalpy calibrations were made by using indium or other organic compounds with known T_m and enthalpy values. A heating rate of 7.5 °C/min was used to assure the thermal equilibrium of the DSC cell. Dry argon was used as the purge gas. The sample weights were 15–20 mg. Scanning from -170 °C gave an excellent baseline for ΔC_p determination. The glass transition temperature was taken as the onset of the phenomena.

Films were tested by dynamic mechanical analysis (DMA) on a Rheometrics Solid Analyzer RSA II apparatus operating at 10 Hz from -150 to +150 °C using a temperature step mode (dimensions of the sample = $24 \times 3 \times 1 \text{ mm}^3$). The dynamic Young's modulus (E' , E'' , and $\tan \delta$) was recorded for all experiments.

Small-angle X-ray measurements were made on samples of 0.8-mm thickness by using a special apparatus. A point collimation was obtained using a point source and a double-curve mirror. The collimation system was adjustable so that the scattering vector q up to $q = 10^{-3} \text{ \AA}^{-1}$ could be measured with the aid of an X-ray rotating anode generator RIGAKU (12 kV) with a copper target. The small-angle X-ray scattering intensities were measured with a position-sensitive detector associated with a multichannel analysis system.

Sample and X-ray beams were under vacuum in order to limit air scattering. On the figures, the scattering intensity $I(q)$ versus the scattering vector q were plotted after subtraction of the background scattering. Small-angle scattering provides a useful means for characterization of the microdomain structure of pseudo-two-phase polymer systems. The continuous scattering in the neighbourhood of the direct beam is related to the existence of heterogeneities in the sample, these heterogeneities having dimensions from several tens to several hundred times that of the X-ray wavelength. The scattered intensity (I) is plotted as a function of q , the magnitude of the scattering vector. By definition

$$q = 4\pi \sin 2\theta / \lambda \quad (4)$$

where λ is the wavelength and 2θ is the scattering angle.

From this assumption, careful analyses of the SAXS curves provide measurements of diffuse boundary thickness, degree of microphase separation, and domain size distribution.

Results and Discussion

Ceramers Based on PDMS. Thermomechanical Analysis. All the synthesized films were colorless and transparent. Figure 1 shows DSC scans for (a) the initial heating run and (b) the heating run after quenching from the melt. The results are given in Table III. The two-phase behavior of the polymers is shown in Figure 1, where two glass transitions are observed. The structure of our ceramer networks is somewhat similar to that of a segmented polyurethane. The soft segments consist of the macrodiol, and the hard units are formed by isophorone diisocyanate and (γ -aminopropyl)triethoxysilane. It should be more complicated because cross-links are formed during polymerization. However during polymerization and in the final polymer, the hard units and the soft segments

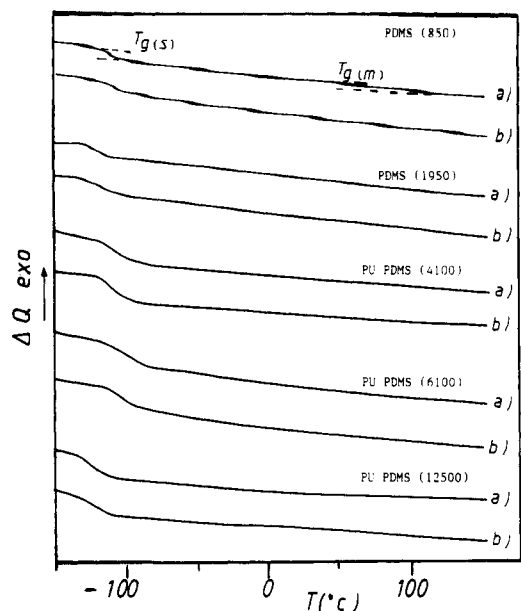


Figure 1. DSC thermograms of PDMS ceramers: (a) first scan; (b) second heating after quenching.

Table III
DSC Measurement Data ($q = 7.5$ °C/min) for PDMS Ceramers

macromonomer	% SS	$T_{g(s)}^o$ (°C)	$T_{g(s)}$ (°C)	$\Delta C_{p(s)}$ [J/(g·K)]	$\Delta C_{p(s)}/\Delta C_{p(s)}^o$
PDMS (850)	49	-118	(a) -115	0.38	0.88–0.92
			(b) -115	0.37	
PDMS (1950)	69	-125	(a) -123	0.39	0.95–0.96
			(b) -122	0.38	
PU PDMS (4100)	87	-125	(a) -113	0.33	0.82–0.85
			(b) -113	0.32	
PU PDMS (6100)	66	-118	(a) -115	0.37	0.86–0.88
			(b) -115	0.36	
PU PDMS (12 500)	88	-125	(a) -125	0.33	0.85–0.87
			(b) -123	0.33	

tend to segregate due to their immiscibility and produce a two-phase material.

The glass transitions at the lower temperature range, $T_{g(s)}$ are from the PDMS-rich phase. The closeness of these $T_{g(s)}$ to the $T_{g(s)}^o$ of hydroxy-terminated PDMS (-125 °C) indicates that phase separation of the soft segment is nearly complete. A quantitative evaluation of the degree of phase segregation in segmented linear polyurethanes is possible by measuring the heat capacity change, ΔC_p , at the glass transition of the soft phase.²⁷ The heat capacity change, $\Delta C_{p(s)}$, per gram of soft segment in the polyurethane is compared with the $\Delta C_{p(s)}^o$ of the pure soft phase measured for the oligomer. $\Delta C_{p(s)}^o$ is equivalent to the ΔC_p per gram of the soft segments at the glass transition in totally phase-separated polymers if restrictions resulting from the incorporation into the polymer are neglected. The ratio $(\Delta C_{p(s)}/\Delta C_{p(s)}^o)$ corresponds to the percentage of segregation of the soft blocks; $\Delta C_{p(s)}^o - \Delta C_{p(s)}$ corresponds to the quantity of soft segments located out of the soft phase and, therefore, in the hard domain or at the interphase. These dispersed soft segments do not relax at the same temperature as in the continuous soft phase.

This calculation is correct only if the soft phase is relatively pure²² which seems to be the case here because $T_{g(s)} \approx T_{g(s)}^o$.

Taking into account the $\Delta C_{p(s)}$ values of the second run, we applied this calculation and determined the percentage of segregation of the soft segments for our ceramers based on PDM. We obtain rather high values of $(\Delta C_{p(s)}/\Delta C_{p(s)}^o) = 0.80$ – 0.90 .

The change of heat capacity of amorphous hard domains at the glass transition is generally too small to be observed

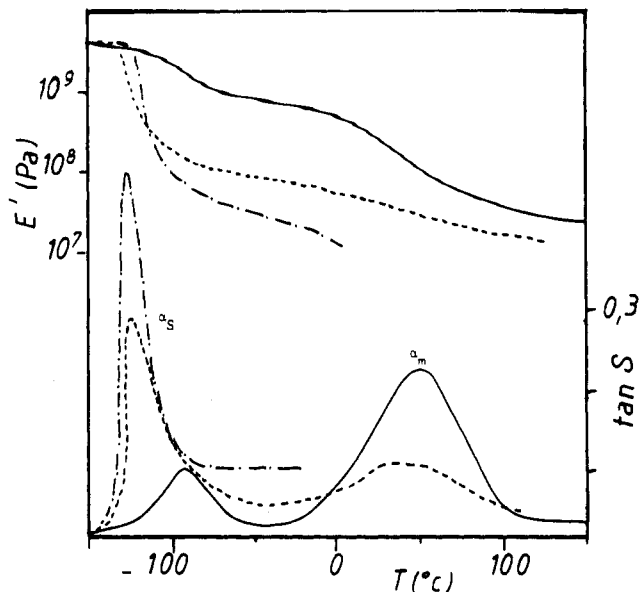


Figure 2. Dynamic mechanical properties of PDMS-based ceramers: (—) PDMS (850); (---) PDMS (1950); (- - -) PU PDMS (4100).

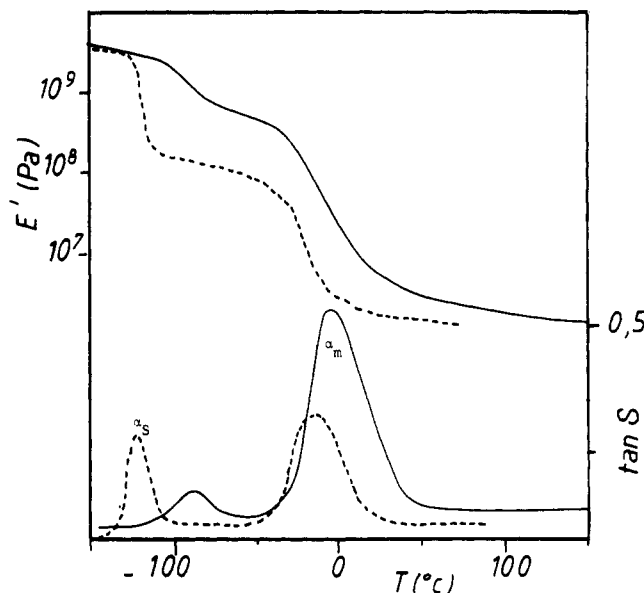


Figure 3. Dynamic mechanical properties of PU PDMS-based ceramers: (—) PU PDMS (6100); (---) PU PDMS (12 500).

Table IV
Dynamic Mechanical Results for PDMS Ceramers (a) at the Maximum of the $\tan \delta$ peak and (b) at $T_{\alpha s} + 50$ °C

sample	% SS	$T_{\alpha s}^a$ (°C)	$h_{\alpha s}$	G'^b (MPa)	$T_{\alpha m}^a$ (°C)	$h_{\alpha m}$
PDMS (850)	49	-89	0.099	638	50	0.23
PDMS (1950)	69	-115	0.29	95	45	0.014
PU PDMS (4100)	87	-115	0.46	38		
PU PDMS (6100)	66	-89	0.12	330	-3	0.56
PU PDMS (12 500)	88	-115	0.25	12	0	0.24

by DSC. In our case, a little variation of ΔC_p is observed between 0 and 100 °C for the PDMS (850) film, but it is too weak to be estimated.

The results of dynamical mechanical testing for PDMS ceramers are displayed in Figures 2 and 3 and Table IV. All transitions were determined from the maximum in the lost tangent, $\tan \delta$. Since the trends in loss modulus E'' follow those of $\tan \delta$, only $\tan \delta$ and storage modulus E' data are shown for purposes.

In Figure 2 the dynamic mechanical spectra of PDMS-based ceramers display two relaxations, characteristic of

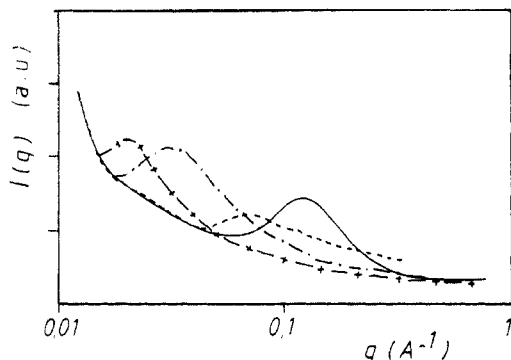


Figure 4. Small-angle X-ray scattering of PDMS-based ceramers: (—) PDMS (850); (---) PDMS (1950); (+ + +) PU PDMS (4100); (- - -) PU PDMS (6100).

a microphase separation: (i) The storage modulus behavior at $-150\text{ }^{\circ}\text{C}$ is what one would expect for a glassy polymer, i.e. about 10^9 Pa . The onset of the first relaxation occurs at $-120\text{ }^{\circ}\text{C}$ for PDMS (1950)- and PDMS (4100)-based ceramers and at $-90\text{ }^{\circ}\text{C}$ for the PDMS (850)-based ceramer, as indicated by the drop in the storage modulus. Moreover, the rubbery plateau after the second relaxation is distinctly higher for low molecular weight. (ii) The low temperature loss peak is attributed to the backbone motion of PDMS chains that accompanies its glass transition. The temperature of the maximum of the $\tan \delta$ peak for the α_s process (T_{α_s}) associated with the glass transition temperature of PDMS segments decreases when the length of PDMS sequences increases. This decrease in transition temperature can be attributed to a reduction of the effect of chain restrictions on the PDMS segments as the PDMS segment length increases. (iii) The second $\tan \delta$ peak is noted α_m . This relaxation spread on a wide range of temperature, the subscript m will be explained later. In contrast to the soft segment relaxation, the position of the maximum relaxation shifts lightly to lower temperatures and the height of $\tan \delta$ of the α_m relaxation decreases in amplitude with increasing PDMS molecular weight. This can be accounted for by the decrease in the weight fraction of the hard segment. (iv) The polyurethane-modified PDMS ceramers show a lower hard segment glass transition, in addition to the increase in the height of the α_m peak. This is indicative of decreased phase purity in these polyurethane-based materials.

Small-Angle X-ray Scattering (SAXS). The two-phase nature of PDMS networks has been strongly implied above from the results of DSC and DMA. In order to confirm the presence and the character of the domain structure, small-angle X-ray analysis was applied to both series of ceramer networks. Figure 4 shows the SAXS curves for the PDMS-based samples. A broad peak is observed in all scattering curves, with the maximum position shifting toward smaller q as the PDMS sequence length increases. Such results strongly imply that a correlation distance exists in these materials, but this parameter is not a well-defined physical dimension of the polymer structure and only indicates qualitatively the scale of the electron density variation related to the microdomain spacing.

Moreover, the electron-density calculations reveal that the cross-link units possess an electron density ($\rho = 0.68\text{ mol of e}^-/\text{cm}^3$) that differs from the electron density of oligomers ($\rho \approx 0.52\text{ mol of e}^-/\text{cm}^3$) or the prepolymers used as soft segments. It is apparent that the SAXS profile reflects the phase contrast between a soft phase and hard phase including cross-link units.

Meier²⁴ has previously shown that the equilibrium domain shape in block copolymers is spherical when the

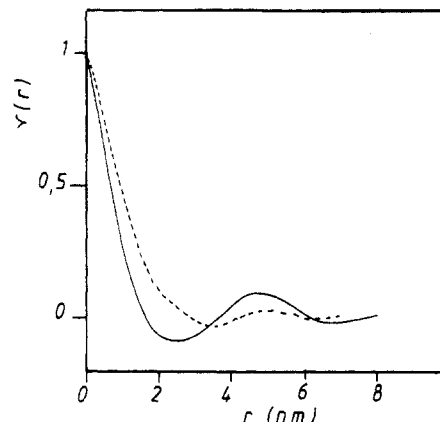


Figure 5. Example of 1- and 3-dimensional correlation function for the PDMS (850) ceramer: (---) 1D; (—) 3D.

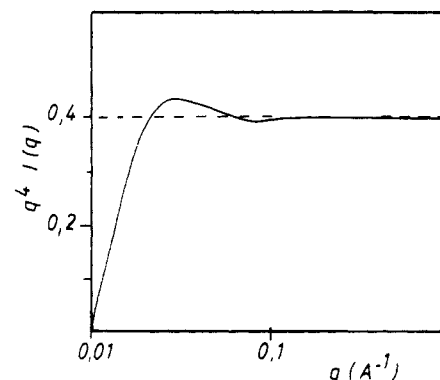


Figure 6. Porod plot for PDMS (850) ceramer.

components are amorphous. It is a reasonable assumption that the siloxane hard segments take the form of spherical inclusions in agreement with previous results.

The correlation function can be determined by the use of the one-dimensional (1-D) correlation function²⁵

$$\gamma(x) = \frac{1}{Q} \int_0^\infty q^2 I(q) \cos(qx) dq \quad (5)$$

or the three-dimensional (3-D) correlation function²⁶

$$\gamma(r) = \frac{1}{Q} \int_0^\infty q^2 I(q) \frac{\sin(qr)}{qr} dq \quad (6)$$

with $Q = \int_0^\infty q^2 I(q) dq$.

A typical plot of the 1-D and the 3-D functions for the sample PDMS (850) is shown in Figure 5. A better existence of periodicity is observed in the 3-D than in the 1-D correlation function, indicating that the morphology of microdomains is rather three-dimensional. To confirm this result, a Porod's law is used:

$$\lim_{q \rightarrow \infty} I_{\text{obs}}(q) = K_p/q^4 \quad (7)$$

where K_p is the Porod's constant.

Thus, for an ideal two-phase system, the product $q^4 I(q)$ should reach a constant value. Figure 6 is a typical Porod's plot of our samples. To have an ideal of the size of the microdomains, we assumed that these microdomains are spherical. So, the volume size distribution function of a particle of diameter D can be calculated from the correlation function by a numerical method:²⁸

$$\gamma(r) = \int_r^\infty F_v(D) \gamma(D)(r) dD \quad (8)$$

where $\gamma(D)$ is the correlation function of a sphere of diameter D and $F_v(D)$ is the volume size distribution function.

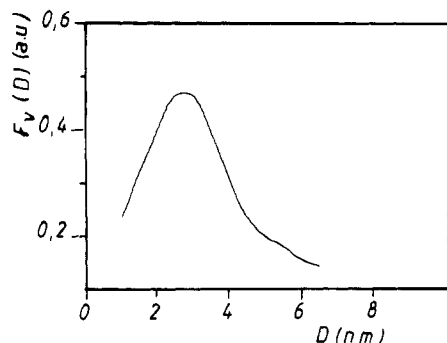


Figure 7. Volume size distribution for the PDMS (850) ceramer calculated from the correlation function.

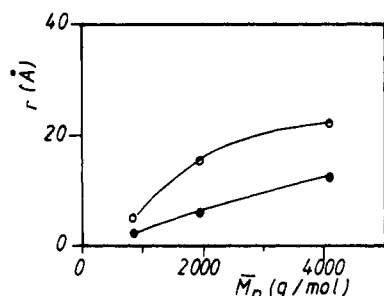


Figure 8. Comparison of the correlation distance from SAXS (O) and the end-to-end distance (●) calculated by the Flory-Fox equation.

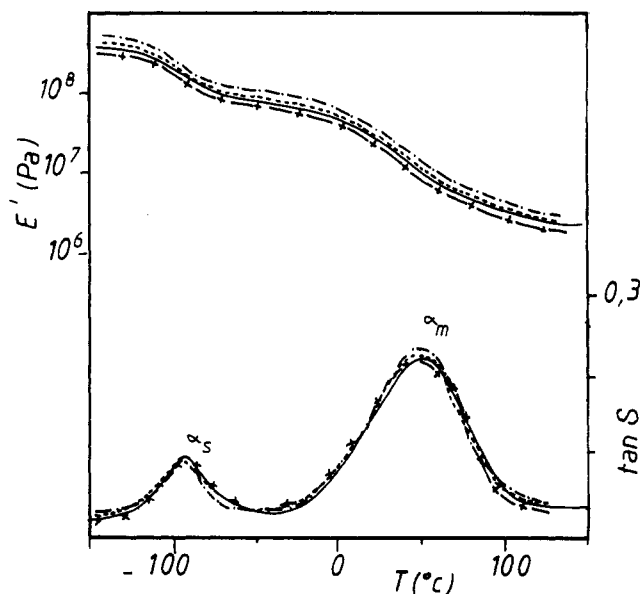


Figure 9. Dynamic mechanical properties of PDMS (850)-based ceramers cured with different isothermal treatments: (—) 12 h at 80 °C; (---) +3 h at 150 °C; (- - -) +12 h at 150 °C; (+ - +) +18 h at 150 °C.

Table V
SAXS Results for PDMS and H-PBD Ceramers

sample	<i>d</i> (nm)	ϕ (nm)
PDMS (850)	5.1	3.0
PDMS (1950)	15.4	3.0
PU PDMS (4100)	22.0	3.0
PU PDMS (6100)	7.0	3.0
H-PBD (2000)	5.5	3.1
PU H-PBD (14 000)	7.5	3.2

One example of the volume size distribution calculation is given in Figure 7. Table V presents the results. In every case, the diameter of the spherical particles is found equal to 3 nm (30 Å).

In order to ascertain the values obtained from this method, the correlation distance of each sample is directly related to the molecular weight of the soft sequence. Figure

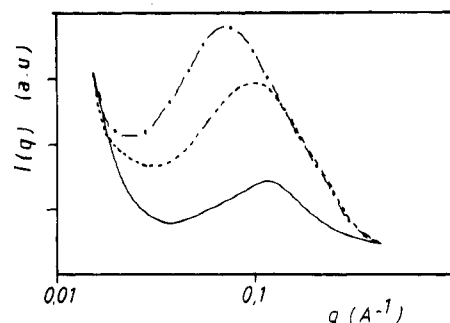


Figure 10. Small-angle X-ray scattering of PDMS (850)-based ceramers cured with different isothermal treatments: (—) 12 h at 80 °C; (---) +3 h at 150 °C; (- - -) +12 h at 150 °C.

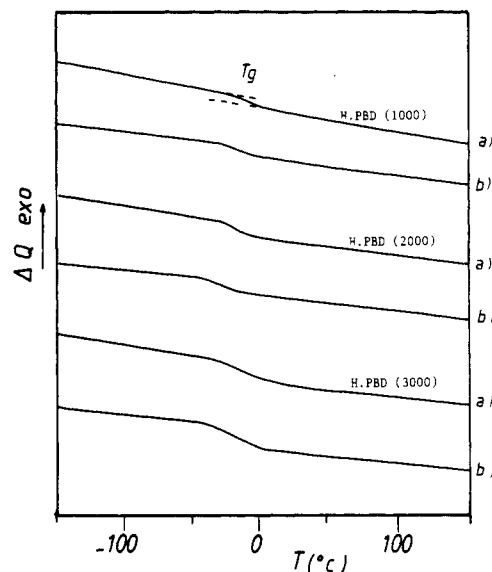


Figure 11. DSC thermograms of H-PBD ceramers: (a) first scan; (b) second heating after quenching.

Table VI
SAXS Results for PDMS-Based Ceramers (Influence of the Aging Time)

postcuring time at 150 °C (h)	<i>d</i> (nm)	ϕ (nm)
0	5.1	3.0
3	5.5	3.5
12	6.7	4.5

Table VII
DSC Measurement Data ($\dot{q} = 7.5$ °C/min) for H-PBD Ceramers

sample	% SS	$T_{g(s)}$ (°C)	$T_{g(a)}$ (°C)	$\Delta C_{p(s)}$ [J/(g·K)]
H-PBD (1000)	53	-46	(a) -28	0.17
			(b) -27	0.16
H-PBD (2000)	69	-45	(a) -28	0.24
			(b) -27	0.24
H-PBD (3000)	77	-43	(a) -25	0.30
			(b) -25	0.29
PU H-PBD (8200)	69	-46	(a) -27	0.25
			(b) -26	0.25
PU H-PBD (14 000)	88	-45	(a) -25	0.32
			(b) -23	0.32

8 shows the dependence of the correlation distance *d* on the molecular weight of the oligomers. We have also represented in this figure the end to end distance of PDMS chains calculated by the following simple equation:

$$\langle r^2 \rangle = Nl^2 \quad (9)$$

with the *r* unperturbed end to end distance of PDMS chains, *N* the number of segments (Si-O), and *l* the length of the Si-O bond.

For the low molecular weight, these two values (correlation distance and end to end distance) are relatively

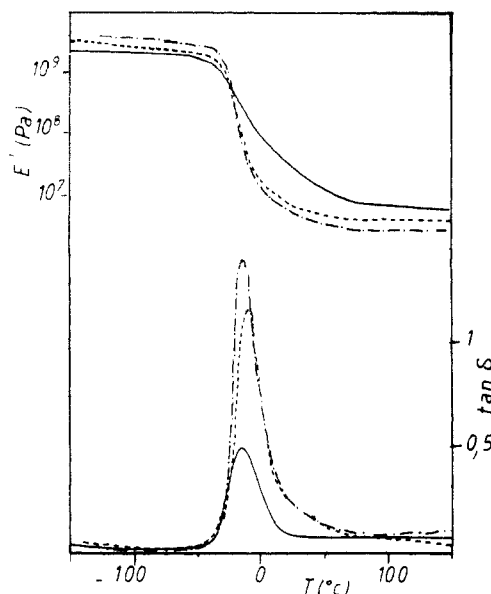


Figure 12. Dynamic mechanical properties of H-PBD-based ceramers: (—) H-PBD (1000); (---) H-PBD (2000); (- · -) H-PBD (3000).

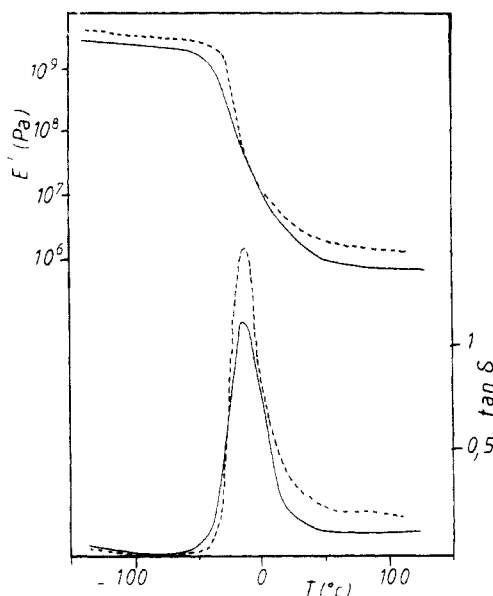


Figure 13. Dynamic mechanical properties of PU H-PBD-based ceramers: (—) PU H-PBD (8200); (---) PU H-PBD (14 000).

close. As the length of PDMS sequences increases, the difference between the two values becomes important. Such a deviation can prove that the model used does not take into account the deviation of the PDMS molecular chains from the Gaussian model and the additional restrictions imposed on rotations of the PDMS Si-O bond.

For the PU-modified PDMS ceramers, the correlation distance between clusters is found equal to 7 nm, while the diameter of spherical particles is still equal to 3 nm. In Figure 4, there is a pronounced difference in the SAXS profile between the PDMS-based materials and the modified PDMS materials. The well-distinguished SAXS peak of the PDMS materials may be attributed to its high degree of phase separation. For the PU-modified PDMS, the PDMS chains are mixed in the hard phase as shown by dynamic mechanical experiments. This may enhance phase mixing and create a lower electron density difference which results in lower scattering intensity (see Figure 4).

Attempt To Describe the Morphology. The two relaxations observed by dynamic mechanical analysis are important in interpreting the experimental results. The phase separation is due to the large degree of immiscibility

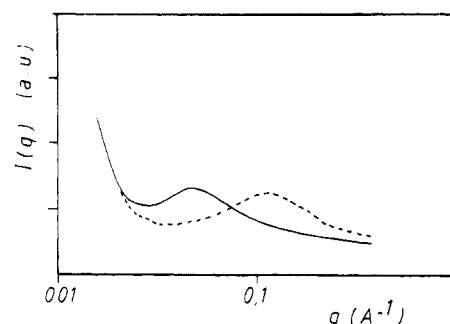
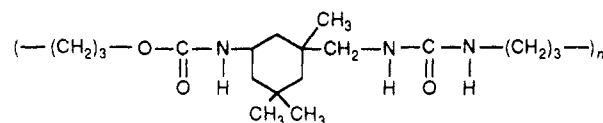


Figure 14. Small-angle X-ray scattering of H-PBD-based ceramers: (—) H-PBD (2000); (---) PU H-PBD (14 000).

Table VIII
Dynamic Mechanical Results for H-PBD-Based Ceramers
(a) at the Maximum of the tan δ peak and (b) at $T_g + 80$ °C

sample	% SS	T_g^a (°C)	h_a	G'^b (MPa)
H-PBD (1000)	53	-15	0.51	7.4
H-PBD (2000)	69	-10	1.15	4.2
H-PBD (3000)	77	-10	1.35	2.6
PU H-PBD (8200)	69	-15	1.12	0.94
PU H-PBD (14 000)	88	-15	1.6	0.52

between the hard and soft units, but as the PDMS oligomer is incorporated into a ceramer network, several possible situations may exist. (i) The oligomer may form a rich PDMS phase whose mobility will not be restrained too much by the cross-links except through the end-linking effect for low-molecular-weight PDMS. This soft phase relaxes at low temperature, near the temperature of the initial PDMS. The α_S relaxation observed is attributed to the soft phase, practically pure in PDMS. (ii) The cross-link units are formed of polysiloxane $>Si-O-Si<$, quasi similar to inorganic silicate which can segregate into clusters before or during cross-link reaction. These clusters may relax at very high temperature, 300–600 °C, and it is not detectable by DMA, due to the thermic stability of the organic chains. On the contrary, SAXS measurements are able to observe the organization of these clusters into microdomains. (iii) PDMS chains are connected to cross-links through urethane-urea units:



As the alkoxy silane condensation reaction is not complete, some chain extension of these units through $>Si-O-Si<$ bonds is also possible.

These units are not miscible with 80–90% of the PDMS chains, neither with inorganic silicate clusters. With 10–20% of the PDMS chains, they formed a mixed phase, or a large interfacial region, between the pure PDMS soft phase and the silicate hard phase. This mixed interfacial region has a large relaxation that we have called α_m . For all samples, the position of the high-temperature relaxation peak is relatively constant, about 50 °C. The height at the peak maximum becomes higher by decreasing the PDMS content.

If we assume that the composition of the mixed interfacial region is the same (same position) for the three samples with PDMS with different molecular weights, decreasing the PDMS content increases the number of urethane-urea units and so increases the mixed interfacial region. The SAXS peak is due to the silicate clusters, but it is difficult to know if it includes the mixed interfacial region.

The inverse of the scattering parameter, d , is the correlation length between two silicate clusters. The

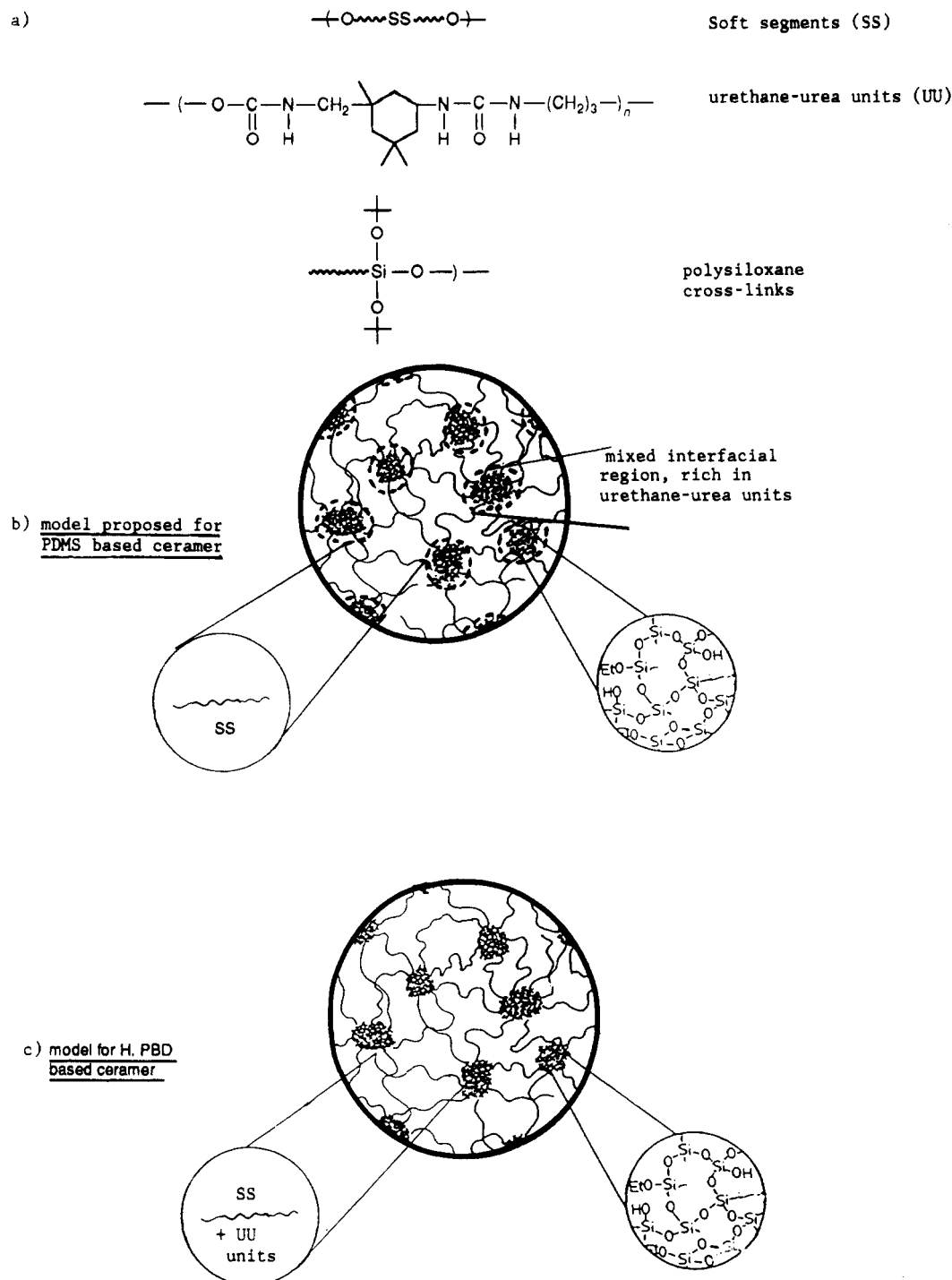


Figure 15. Schematic model for the structure of H-PBD-based ceramers:¹⁵ (a) segment units and cross-links; (b) model proposed by PDMS-based ceramers; (c) model for H-PBD-based ceramers.

correlation distance observed by SAXS is expected to be of the order of the end to end distance of the oligomer or copolymer used. Experimentally, we observe that the correlation distance increases with an increase in PDMS sequence length but is higher than the expected unperturbed end-to-end distance.

Moreover, the alkoxyisilane groups are not completely condensed, as we have shown in previous work.²³ In order to investigate the influence of the curing process on the material properties, we have compared the networks obtained by solution or bulk polymerization. Films obtained by solution polymerization are transparent too. For example, in the dynamic mechanical spectra of PDMS (850), obtained by the two different ways, the behavior of the storage modulus and loss tangent is similar for both cases. The type of synthesis does not affect the thermal and mechanical properties either. The good point of bulk

synthesis is to reduce the time necessary to obtain identical ceramer networks (12 h at 80 °C instead of 1 week under ambient conditions).

Different isothermal postcured treatments were carried out at $T_c = 150$ °C on the PDMS (850) sample synthesized in bulk. All treatments result in the same value of the glass transition temperature of the soft sequence T_{gs} (−88 °C) and the same value of $T_{\alpha H} \sim 50$ °C, as we can see in Figure 9. The storage modulus increases slightly with the thermal treatment, before decreasing after 18 h at 150 °C.

This last effect may be explained by thermal degradation, while the increase in modulus before can be explained by the pursuit of some condensation reactions of residual alkoxyisilane groups. This can be understood in terms of the structural model suggested earlier. The clusters which serve as the connecting sites for PDMS chains are expected to contain unreacted ethoxy and silanol groups that can

Table IX
Solubility Parameters of the Different Components of Networks

component	chemical structure	δ (MPa ^{1/2})
PDMS		15.3
H-PBD		16.2
IPDI		21.6
γ -APS		17
urethane-urea unit in PDMS		23.5
urethane-urea unit in H-PBD		21.5
polysiloxane cross-link		42

undergo further condensation with time.

SAXS was employed to study the structural changes in the PDMS (850) ceramer as a function of aging time at high temperature (see Figure 10 and Table VI). The resulting data show an increase in the scattering intensity and in the correlation distance with the aging time. We have to keep in mind that the initial isothermal treatment of our samples is done at a temperature of 80 °C and that the transition temperature T_{am} is between 0 and 100 °C, with the maximum of $\tan \alpha_m$ at about 50 °C. Since we have an immiscible system, phase separation is stopped by the vitrification of the mixed phase and the hard phase and we have a multiphase system which is not in equilibrium. At a lower $\Delta T = T_c - T_{as}$, the rate of rearrangements is low but it increases when ΔT increases. Since the observed scattering intensity is related to the electron density difference between the cluster and the oligomer-rich region, the scattering intensity should increase as the purity of the soft phase increases with aging.

Thermal treatments change the morphology for the most part and not the phase composition. The fact that, during thermal treatments, the relaxation peaks do not change significantly but only the correlation length is changing is consistent with the fact that, (i) by DMA, the relaxations of the soft and interfacial regions are observed and, (ii) by SAXS, the distance between clusters is determined. It is not possible to measure the increase of the cross-link density by the two techniques.

Ceramers Based on H-PBD. Thermomechanical Analysis. Differential scanning calorimetry curves of H-PBD-based materials are shown in Figure 11. The thermal transition data are summarized in Table VII. It appears that the molecular weight of H-PBD in the range studied ($M_n \geq 1000$) does not have a great influence on the glass transition temperature of the material. Moreover, the DSC data show that the H-PBD-based ceramers have one T_g and this T_g (−30 °C) is 10–15 deg higher than that of the initial H-PBD oligomer (−45 °C).

Figures 12 and 13 show the dynamic spectra of materials based on H-PBD. Direct comparison of PDMS and H-PBD spectra shows higher storage moduli in the H-PBD materials. With regard to the $\tan \delta$ behavior, the difference between these two types of oligomers is rather significant. A single peak, instead of a bimodal behavior shown by the PDMS samples, is observed for the H-PBD-based materials, and the magnitude of the relaxation is always higher than that of the PDMS-based ceramers. In agreement with the DSC results, the a peak of the E' curves, which is attributed to the glass transition of the soft phase, shifts several degrees Celsius in the different materials. The results concerning H-PBD materials are compiled in Table VIII.

In any case, the general behavior of the storage modulus is similar for all H-PBD samples: first, a glassy region which shows a magnitude of 10^9 Pa, followed by a transition region to the rubbery state near −15 °C. The transition in E' from the glassy to the rubbery region is more gradual for the low-molecular-weight H-PBD materials as compared to the higher molecular weight and the modified H-PBD samples. It can be seen that as the soft segment content is decreased, the value of the modulus corresponding to the rubbery plateau is increased but the position of the relaxation peak is roughly constant. We notice that the temperature position of this relaxation is intermediary between the two relaxations α_S and α_m observed for PDMS ceramers.

SAXS Results. SAXS profiles of the H-PBD (2000) and PU H-PBD (14 000) materials are shown in Figure 14. Even if we have one transition and one relaxation, each scattering profile exhibits a scattering peak, characteristic of a periodic variation in electron density within the sample.

As suggested above, both ends of an end-capped H-PBD chain are believed to be connected to the final network by the condensed alkoxy silane cross-link points. As we can see in Table V, the diameter of these spherical particles

is identical to these obtained for PDMS samples (o.d. = 3 nm). The correlation distance of the H-PBD (2000) sample is related to the molecular weight of the soft sequences. The unperturbed end to end distance of H-PBD chains is calculated with the equation (9) previously used.

The correlation distance ($d = 5$ nm) and the end to end distance ($r = 5.5$ nm) are relatively close and confirm our hypothesis.

Discussion and Conclusion

The structure of PDMS- and HPBD-based ceramers have to be compared.

The molecular structure of our ceramer networks is similar to that of a cross-linked segmented polymer formed of different constitutive units (Figure 15a): (i) the soft segment with different composition, PDMS or H-PBD and different molecular weight, (ii) the urethane-urea (UU) units used to link the soft segment to the alkoxyisilane groups, and (iii) the condensed alkoxyisilane or silanol cross-links.

The three types of constitutive units are quite immiscible in the case of PDMS-based ceramers. This immiscibility is confirmed by their different solubility parameters (Table IX). DMA and SAXS results can be explained by a three-phase system responsible for different relaxations and a scattering peak: (i) one soft phase, containing practically pure PDMS ($T_{g(s)} \approx T_{g(s)}^0$ and given a relaxation α_s at low temperature, (ii) one hard phase, formed from silicate cross-links (The relaxation of this phase is not detectable by DMA because it is at too high a temperature where the polymer is not stable. However this phase gives a scattering peak by SAXS and a correlation length), and (iii) a third phase we have called a mixed interfacial region which can explain the second relaxation α_m observed by DMA (This phase contains around 10–20% of the PDMS and most of the urethane-urea units. The structure of the polymer obliged this mixed phase to be between the soft and the hard phase; this is why it can also be called interfacial phase).

Wilkes et al.¹⁵ previously proposed a schematic model for these heterogeneous networks. We use this model to represent the morphology of our PDMS-based ceramer (Figure 15b).

Compared to PDMS-based ceramers, H-PBD-based ceramers have a similar SAXS profile, indicating a multiphase material but only one relaxation, 10–20 deg higher than the relaxation of the initial H-PBD oligomers. This is consistent with the fact that in this case we have only two phases: (i) a soft phase rich in H-PBD, but containing also the urethane-urea units (ii) and a hard phase formed as previously from silicate cross-links. The fact that the correlation lengths are in the same range of value for the two types of ceramers is consistent with our attribution.

The fact that the soft segments and urethane-urea units are miscible in the case of H-PBD and not with PDMS can be explained by the different solubility parameters. The immiscibility of PDMS segments is well-known in the literature. Wilkes et al.²⁹ for example have prepared two phase polymers by chain extending the same type of

PDMS with a diisocyanate. Another example is the work of Cooper et al.³⁰ on PDMS cross-linked by reaction of double bonds introduced at each end.

Comparatively, the schematic structure of H-PBD-based ceramers is given in Figure 15c. Comparison with other morphological results on ceramers is difficult because tetraethoxysilane (TEOS) is generally used as an additive. Even then it seems that in the case of PTMO-based ceramers, Wilkes et al.¹⁵ also observed a three-phase systems, but with a very large mixed interfacial region. Our systems seem to be better models to understand the complex morphology of hybrid networks.

Acknowledgment. This work was sponsored by the Corning Europe Co. The financial support of this institution is gratefully acknowledged. We also wish to thank J. Perez from GEMPPM (INSA-LYON) for stimulating discussion.

References and Notes

- Hoh, K. P.; Ishida, H.; Koenig, J. L. *Polym. Comp.* **1990**, *11*, 121.
- Serier, A.; Pascault, J. P.; Lam, T. M. *J. Polym. Sci., Polym. Chem.* **1991**, *29*, 1125.
- Livage, J.; Henry, M.; Sanchez, C. *Prog. Solid State Chem.* **1988**, *18*, 259.
- Keefer, K. D. *Mater. Res. Soc. Symp. Proc.* **1984**, *32*, 15.
- Schmidt, H. *Mater. Res. Soc. Symp. Proc.* **1984**, *32*, 327.
- Schmidt, H.; Seiferling, B. *Mater. Res. Soc. Symp. Proc.* **1986**, *73*, 739.
- Ravaine, D.; Seminel, A.; Charbouillot, Y.; Vincens, M. *J. Non-Cryst. Solids* **1986**, *82*, 210.
- Fujita, M.; Honda, K. *Polym. Commun.* **1989**, *30*, 200.
- Spindler, R.; Shriver, D. F. *Macromolecules* **1988**, *21*, 648.
- Levy, D.; Einhorn, S.; Avnir, D. *J. Non-Cryst. Solids* **1989**, *113*, 1137.
- Kohjiya, S.; Ochiai, K.; Yamashita, S. *J. Non-Cryst. Solids* **1990**, *119*, 132.
- Huang, H. H.; Orler, B.; Wilkes, G. L. *Polym. Bull.* **1985**, *14*, 557.
- Huang, H. H.; Orler, B.; Wilkes, G. L. *Macromolecules* **1987**, *20*, 1322.
- Brennan, A. B.; Wilkes, G. L. *Polymer* **1991**, *32*, 733.
- Huang, H. H.; Wilkes, G. L. *Polym. Bull.* **1987**, *18*, 455.
- Huang, H. H.; Glaser, R. H.; Wilkes, G. L. *Polym. Prepr., Am. Chem. Soc. Div. Polym. Chem.* **1987**, *28*, 434.
- Huang, H. H.; Wilkes, G. L.; Carlson, J. G. *Polymer* **1989**, *30*, 2001.
- Noell, J. L. W.; Wilkes, G. L.; Mohanty, D. K.; Mac Grath, J. E. *J. Appl. Polym. Sci.* **1990**, *40*, 1177.
- Enns, J. B.; Gillham, J. K. *J. Appl. Polym. Sci.* **1983**, *28*, 2567.
- Surivet, F.; Lam, T. M.; Pascault, J. P. *J. Polym. Sci., Polym. Chem.* **1991**, *29*, 1977.
- Wang, C. Z.; Li, C.; Copper, S. L. *J. Polym. Sci., Polym. Phys.* **1991**, *29*, 75.
- Cuve, L.; Pascault, J. P.; Boiteux, G.; Seytre, G. *Polymer* **1991**, *32*, 343.
- Surivet, F.; Lam, T. M.; Pham, Q. T.; Pascault, J. P. To be published (part 1).
- Meier, D. J., *J. Polym. Sci., Part C* **1969**, *26*, 81.
- Debye, P.; Bueche, A. M. *J. Appl. Phys.* **1949**, *20*, 518.
- Vonk, C. G.; Kortleve, G. *Kolloid Z.* **1967**, *19*, 220.
- Camberlin, Y.; Pascault, J. P. *J. Polym. Sci., Polym. Physics Ed.* **1984**, *22*, 1835.
- Mai, C.; Livet, F.; Vigier, G. *Scr. Metall.* **1981**, *15*, 1179.
- Tyagi, D.; Ylgor, I.; MacGrath, J. E.; Wilkes, G. L. *Polymer* **1984**, *25*, 1807.
- Yu, X.; Nagarajan, M. R.; Speckhard, T. A.; Cooper, S. L. *J. Appl. Polym. Sci.* **1985**, *30*, 2155.